Retrospective Gating vs. Prospective Triggering for Noninvasive Coronary Angiography:

Assessment of Image Quality and Radiation Dose Using a 256-Slice CT Scanner with 270 ms Gantry Rotation

Wei-Yip Law, MD, Ching-Ching Yang, PhD, Liang-Kuang Chen, MD, Tzung-Chi Huang, PhD, Kun-Mu Lu, BS, Tung-Hsin Wu, PhD, Greta S. P. Mok, PhD

Objective: To report our clinical experience with a 256-slice multidetector computed tomography (MDCT) with a 270-ms gantry rotation system in performing CT coronary angiograms (CTCA) using both prospectively gated step and shoot (PGSS) and retrospectively gated helical (RGH) techniques.

Materials and Methods: We studied 252 patients who received CTCA; 126 patients having mean heart rate (HR) of 72.1 were imaged with RGH CTCA and 126 patients having mean HR of 58.7 were imaged with PGSS CTCA. For patients with a prescan HR ≤70 beats/min, a PGSS acquisitions trigger was used, whereas patients whose prescan HR was >70 beats/min were imaged using an RGH acquisition. The blood vessel accessibility of both PGSS and RGH techniques was evaluated by grading the image quality score from 1 (no motion artifacts) to 4 (severe motion artifacts preventing diagnosis) for each coronary artery segment. Radiation doses of the techniques were also compared.

Results: In both groups, more than 50% of segments received the best imaging score. The overall image quality scores for RGH and PGSS groups were 1.522 ± 0.317 and 1.500 ± 0.374, respectively. There was no significant difference in right coronary artery, left anterior descending artery, and left circumflex artery image quality between the two groups. Only 0.1% of segments were nonevaluative with the PGSS technique and all segments were evaluative with RGH. PGSS was associated with a 62% reduction in effective radiation dose as compared to RGH (PGSS, 5.1 mSv; RGH, 13.2 mSv).

Conclusions: There is no significant difference in image quality between PGSS and RGH in this study. Although providing similar image quality as RGH, PGSS was associated with a 62% reduction in effective radiation dose. Further study to confirm the diagnostic accuracy as compared to coronary artery angiography is warranted.

Key Words: Coronary angiography; CT coronary angiogram; coronary artery disease; CTCA; radiation dose.

©AUR, 2011

Computed tomography coronary angiography (CTCA) using 64-slice multidetector computed tomography (MDCT) and dual-source CT (DSCT) is highly accurate for the detection of coronary artery disease (CAD). Although the noninvasive nature of CT is attractive, the radiation dose of CTCA compared to catheterization remains a significant hurdle because doses for conventional coronary angiography range from 5 to 12 mSv (1), whereas those of retrospectively gated helical (RGH) CTCA range from 12 to 28 mSv (2,3).

With RGH, image data are acquired continuously throughout the cardiac cycle and the reconstruction phase with the least amount of motion artifact is retrospectively chosen, usually during ventricular diastole (4). On the other hand, prospectively gated step and shoot (PGSS) is a CT acquisition technique in which x-rays are turned on only during the cardiac phase of interest. Being prospective in nature, PGSS requires precise synchronization of the x-ray with the cardiac cycle, and its successful implementation also depends on the matching between the selected phase of the cardiac cycle and the phase with least motion. The continuous application of radiation throughout the cardiac cycle with RGH results in a higher radiation dose as compared to PGSS (5).

Acad Radiol 2011; 18:31–39

Department of Radiology, Shin Kong Wu Ho-Su Memorial Hospital, Taipei, Taiwan, R.O.C. (W.-Y.L, L.-K.C., K.-M.L.); Department of Radiological Technology, Tzu Chi college of Technology, Hualien, Taiwan, R.O.C. (C.-C.Y.); College of Medicine, Fu Jen Catholic University, Taipei, Taiwan, R.O.C. (L.-K.C.); Department of Biomedical Imaging and Radiological Science, China Medical University, Taiwan, R.O.C. (T.-C.H.); Department of Biomedical Imaging and Radiological Sciences, National Yang Ming University, 155 Li-Nong St., Sec. 2, Taipei, Taiwan 112, R.O.C. (T.-H.W.); Department of Electrical and Electronics Engineering, Faculty of Science and Technology, University of Macau, Macau; and Department of Health Technology and Informatics, The Hong Kong Polytechnic University, Hong Kong (G.S.P.M.).
Received May 25, 2010; accepted July 28, 2010. This study was financially supported by the National Science Council of Taiwan (NSC96-2321-B-040-005-MY3). **Address correspondence to:** T.-H.W. e-mail: tung@ym.edu.tw

©AUR, 2011
doi:10.1016/j.acra.2010.07.013

Studies have demonstrated mean effective radiation doses ranging from 2.1 to 6.2 mSv (6–8) with PGSS scanning, which results in a substantial reduction in dose of 52% to 85% (6–10). A recent study showed that for a 128-slice DSCT using the low-dose PGSS and prospectively gated high-pitch protocols, the effective dose can be even lowered to 1.4 mSv and 0.9 mSv, respectively (11). However, studies suggest that PGSS CTCA using the current 64- and 128-slice MDCT and DSCT remain limited by heart rate (HR), heart rate variability (HRV), and body mass index (BMI) (10). Currently, PGSS 64-slice MDCT and DSCT are limited to patients with HRs <63 beats/min (7) and <75 beats/min (8,10,12), respectively, though a recent report by Xu et al (13) indicated DSCT adaptive sequential scan produced a similar image quality as RGH for patients with a HR of 70–110 beats/min.

The recent introduction of the 256-slice MDCT scanner (Brilliance iCT; Philips Medical Systems, Eindhoven, Netherlands) with a 270-ms gantry rotation, 120 kW x-ray tube, and an 80.0-mm detector array has allowed a larger z-axial coverage, where the average acquisition time for a cardiac scan length of 120 mm is <5 seconds for RGH and <3.5 seconds for PGSS. In this study, we compared the image quality, radiation dose, and blood vessel accessibility (6) for CTCA obtained on the 256-slice MDCT scanner using both PGSS and RGH techniques.

MATERIALS AND METHODS

Study Population

The study protocol was approved by the Institutional Review Board of our hospital, and the need for informed consent was waived. It was a retrospective study and we reviewed the hospital database for patients who received CTCA between January 2009 and April 2009 and selected 252 patients consecutively; 126 patients who had received RGH CTCA and 126 patients who had received PGSS CTCA. Patients were excluded for the exam if they reported any history of arrhythmia, allergy to iodinated contrast media, insufficient renal function (creatinine level >1.5 mg/dL), or were pregnant. Most CTCA scans were performed as part of cardiovascular screening for substantial CAD, although additional indications included evaluation of chest pain, tachycardia, positive stress test, elevated cardiovascular risk, and history of coronary bypass or coronary stent placement. No patients with former coronary artery bypass graft surgeries were included for this particular study.

The 256-slice MDCT Protocol

All CTCA examinations were performed using the Brilliance iCT 256-slice CT scanner. Scanning was conducted in a craniocaudal direction covering a region approximately 1 cm caudal to the tracheal bifurcation to the level of the diaphragm. For both RGH and PGSS studies, the scanning delay was determined using an automatic bolus tracking technique. A single unenhanced scan was obtained at the level of the aortic root. This scan was used to place a 10-mm diameter circular region of interest inside the lumen of the ascending aorta. Then, nonionic contrast medium (Optiray 350, Tyco Healthcare, Montreal, Quebec, Canada) was injected to the patients based on the weight (1 mL/kg) and HR (for HR <60 beats/min, 5 mL less and for HR >80 beats/min, 5 mL more) of the patients (ie, 70–90 mL was injected) at a flow rate of 5 mL/second, followed by a 25-mL bolus of saline at the same rate using a dual-head injector (Optivantage, Mallinckrodt, Taco Healthcare, Montreal, Quebec, Canada). About 16 seconds (range 11–23 seconds) after the intensity in the region of interest exceeded 110 Hounsfield units, inspiratory breath-hold scanning was initiated. The 256-slice scanner incorporates real-time arrhythmia management capability that enables the x-ray acquisition to be paused on the detection of ectopy during a PGSS scan and resumed at the same axial location once normal sinus rhythm has returned. This capability was enabled during PGSS scans.

Images were reconstructed with a slice thickness of 0.9 mm, a reconstruction increment of 0.5 mm (10,17), and a medium soft-tissue convolution kernel. The reconstructed matrix size was 512 × 512. The field of view was manually adjusted to encompass the heart. All images were transferred to a separate workstation equipped with postprocessing software (Extended Brilliance Workspace 4.0; Philips).

To increase patient throughput, beta-blockers were not administered unless the patient's HR was >90 beats/min before CTCA. Those patients were administered 40 mg of propranolol orally after the scout scans and returned for CTCA after their HR decreased to <90 beats/min. The assignment of the patients to the imaging protocol was not randomized, but rather was based on the patients' HR. For all patients with a prescan HR ≤70 beats/min, a PGSS acquisitions trigger centered at 75% ± 5% phase tolerance of the R-R interval (ie, cardiac cycle). Patients whose prescan HR was >70 beats/min were imaged with RGH acquisitions.

The acquisition parameters for both PGSS and RGH acquisition protocols are summarized in Table 1. For both RGH and PGSS acquisition, the following parameters were used: 128 × 0.625 mm detector collimation, 256 × 0.625 mm slice collimation by means of a dynamic z-focal spot for double sampling, and 270 ms gantry rotation time. Applying the common half-scan reconstruction techniques allowed a minimum temporal resolution of up to 135 ms. HR-dependent pitch was set at 0.16 for patients with HR ≤62 beats/min and 0.18 for patients with HR >62 beats/min. The tube voltage was 120 kV and an effective tube current of between 471 mA to 860 mAs was applied according to the patient's body weight. To produce the best possible image quality with the RGH technique, electrocardiogram (ECG)-based tube current modulation was turned off for all patients. This decision was made to guarantee a critical comparison of image quality between RGH and PGSS acquisitions.

TABLE 1. Patient Demographic and RGH and PGSS Technical Data

	RGH (n = 126)	PGSS (n = 126)	P Value
Age (y)	56.5 ± 9.8	58.0 ± 8.0	.190
Male gender	77 (61.1)	69 (78.4)	.007*
Body mass index (kg/m^2)	25.6 ± 4.0	25.5 ± 3.3	.930
MHR (beats/min)	72.1 ± 6.9	58.7 ± 7.3	<.001*
HRV (beats/min)	1.3 ± 0.7	1.0 ± 0.8	<.001*
Received beta-blockers	35 (27.8)	5 (5.7)	<.001*
Tube voltage (kV)	120	120	N/A
Tube current (mA)	565.7 ± 91.7	780.3 ± 97.8	<.001*
Scan time (seconds)	4.9 ± 0.3	3.9 ± 1.4	<.001*
Number of shots	Continuous exposure	2–3	N/A
$CTDI_{vol}$ (mGy)	60.0 ± 10.5	22.9 ± 3.1	<.001*
Scan length (mm)	129.7 ± 13.8	131.7 ± 15.6	.300
Effective dose (mSv)	13.2 ± 2.7	5.1 ± 0.9	<.001*

$CTDI_{vol}$, volume computed tomography dose index; HRV, heart rate variability; MHR, mean heart rate; PGSS, prospectively gated step and shoot; RGH, retrospectively gated helical.

Data are presented as mean ± standard deviation for continuous variables and number (percentage) for categorical variables.

*Significantly different, $P < .05$.

CT Data Analysis

Coronary arteries were classified into 15 segments according to the scheme proposed by the American Heart Association (14) and the intermediate artery was designated segment 16, if present. Coronary artery analysis was performed on all vessels with a luminal diameter at the origin of at least 1.0 mm, as measured on the CT data. Images were analyzed and graded randomly by two independent cardiovascular radiologists, each with >5 years' experience, who were blinded to HR, HRV, BMI, and scan types. To estimate HRV, the length of each heart beat during data acquisition was measured for each patient and HRV was then calculated as the standard deviation (SD) from the mean HR (MHR) (15). Images included transverse source images, (curved) multiplanar reformations, thin-slab maximum intensity projections, and volume-rendering mode, and were presented to the observers to identify coronary image quality. After the optimal reconstruction interval was determined, we used motion artifact as the figure of merit for assessing image quality. We performed semiquantitative analysis by using a 4-point ranking scale as follows: 1 = no motion artifacts and clear delineation of the segment; 2 = minor artifacts and mild blurring of the segment; 3 = moderate artifacts and moderate blurring without structure discontinuity; and 4 = severe artifacts and doubling or discontinuity in the course of the segment. A score of 3 or lower was considered acceptable for routine clinical diagnostic purposes. For any disagreement in data assessment, the two readers reviewed the data together until consensus was obtained.

Radiation Dose

Radiation dose estimates were determined using the volume CT dose index ($CTDI_{vol}$) in Gy, as provided on the scanner console, and effective dose was expressed in mSv. The dose-length product is defined as the volume CT dose index multiplied by scan length, and is an indicator of the integrated radiation dose of an entire CT examination. An approximation of the effective dose was obtained by multiplying the dose-length product by a conversion factor, k (= 0.017 mSv/mGy^{-1}/cm^{-1}) (5).

Statistical Analysis

Data were presented as mean ± SD for continuous variables and number (percentage) for categorical variables. Comparisons between the PGSS and RGH techniques were performed by two-sample t-test for continuous covariates and by χ^2 test for categorical variables. Wilcoxon signed-rank test was used to evaluate the difference in the image quality between PGSS and RGH techniques for all segments together and separately for each vessel. Pearson's correlation analysis was performed to estimate strength of correlations between motion scores of all segments and MHR and HRV. Five levels of Pearson's correlation coefficient (r) are defined as: very weak ($r \leq 0.2$); weak ($0.2 < r \leq 0.4$); moderate ($0.4 < r \leq 0.6$), strong ($0.6 < r \leq 0.8$), and very strong ($r > 0.8$). All statistical analyses were performed with NCSS statistical software, version 2007 (NCSS; Kaysville, UT). A two-tailed P value of <.05 was considered statistically significant.

RESULTS

The characteristics of the 252 patients, 126 in the RGH group and 126 in the PGSS group, are shown in Table 1. The two groups were similar in age, BMI, tube voltage, and scan length (all $P > .05$). There were, however, more males ($P = .007$) are in the PGSS group, and a larger tube current was used ($P < .001$). MHR, HRV, scan time, $CTDI_{vol}$, and effective dose in the RGH group were significantly greater than those in

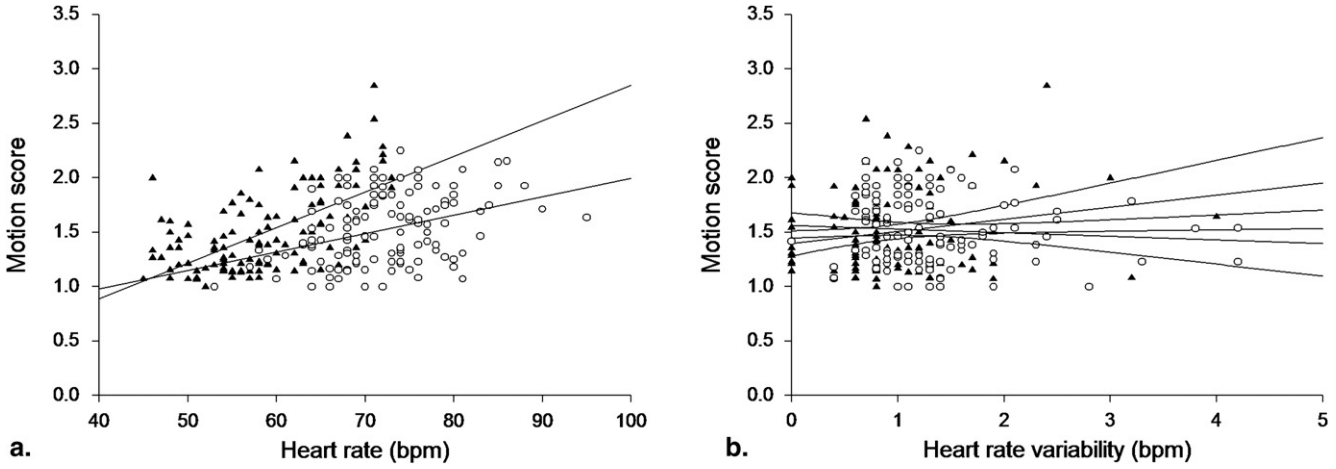

Figure 1. **(a)** Scatter plot of heart rate in retrospectively gated helical (RGH) group ($r = 0.39$, $P < .001$) and prospectively gated step and shoot (PGSS) group ($r = 0.63$, $P < .001$) as against the motion scores. **(b)** Scatter plot of heart rate variability in RGH group ($r = -0.07$, $P = .43$) and PGSS group ($r = 0.20$, $P = .07$) as against the motion scores. *Hollow circles* indicate data for RGH, *solid triangles* indicate data for PGSS, and *lines* represent linear regression model. The image quality was degraded with increasing heart rate for both scan types. *Curves* represent 95% confidence intervals of estimated motion score.

the PGSS group (all $P < .001$). Additionally, as expected, more patients in RGH group with a prescan HR >70 beats/min received propranolol (27.8% vs. 5.7%, $P < .001$).

The correlations between motion score and HR and HRV are illustrated in Figure 1. Except for the correlation between motion score and HR in the PGSS group ($r = 0.72$, $P < .001$), only weak correlations were found for HR in the RGH group. Furthermore, the correlation between the motion score and the HRV was not significant regardless of technique.

Examples of representative images and corresponding scores are presented in Figure 2, and the image quality scores of the two techniques are presented in Table 2. In addition, representative diagnostic images using RGH and PGSS are presented in Figures 3 and 4, respectively. Overall, 50.6% and 54.2% of segments received a score of 1 (best quality image) for PGSS and RGH techniques, respectively, and notably, 0% and 0.1% of coronary segments were nonevaluative (score = 4) in the RGH and PGSS groups, respectively. There was no difference in right coronary artery, left anterior descending coronary artery, and left circumflex coronary artery image quality between the two groups (all, $P > .05$, Table 3). The mean DLP was 301.6 mGy/cm and 778.8 mGy/cm for the PGSS group and RGH group, respectively. Additionally, although providing similar image quality as RGH, PGSS was associated with a 62% reduction in effective radiation dose (RGH, 13.2 mSv; PGSS, 5.1 mSv; Table 1).

DISCUSSION

With technical advances provided by the recently introduced 256-slice CT scanner, such as faster gantry rotation times, larger z-coverage, and increased x-ray tube power, this device is potentially able to image patients with higher HRs and HRV, though its temporal resolution is still inferior to that of the DSCT (16). Because the scan times with the 256-slice CT are substantially shorter, it reduces the susceptibility to ectopy and HRV. Only weak correlations were found for HR in the RGH group and no significant correlation was found between the motion score and the HRV for both acquisition techniques.

In this study, we found that more than 50% of segments received the best imaging quality (score of 1) for both the PGSS and RGH techniques, and approximately the same image quality was obtained regardless of technique. There was no difference in right coronary artery, left anterior descending coronary artery, and left circumflex coronary artery image quality between the two groups, and although providing a similar image quality as RGH, PGSS was associated with a 62% reduction in effective radiation dose. This finding is in agreement with that of Efstathopoulos et al (17), who found a radiation dose of 3.2 ± 0.6 mSv with PGSS 256-slice CTCA and 13.4 ± 2.7 with RGH. The dose associated with PGSS is even lower than that of the RGH technique with an optimal ECG pulsing window for low HR patients (ie, 6.8 mSv), as reported by Weustink et al (18). The radiation dose with PGSS is comparable to, or even lower than, doses associated with conventional coronary angiography, which range from 5 to 12 mSv (1). Further dose reduction is feasible when employing the new proposed prospective helical acquisition mode (19), which is achieved by increasing the pitch (from ~0.2 to 0.27) and avoiding exposure-intensive overscanning, and its full effectiveness requires more investigations (20). Although the dose reduction from the prospective acquisition technique is attractive, the merit of the RGH technique is able to evaluate cardiac functions (eg, wall motion, systolic thickening, left ventricle ejection fraction), leading to a better estimation of prognosis or therapeutic strategy for some patients. Also, the RGH technique can be combined with ECG-controlled tube

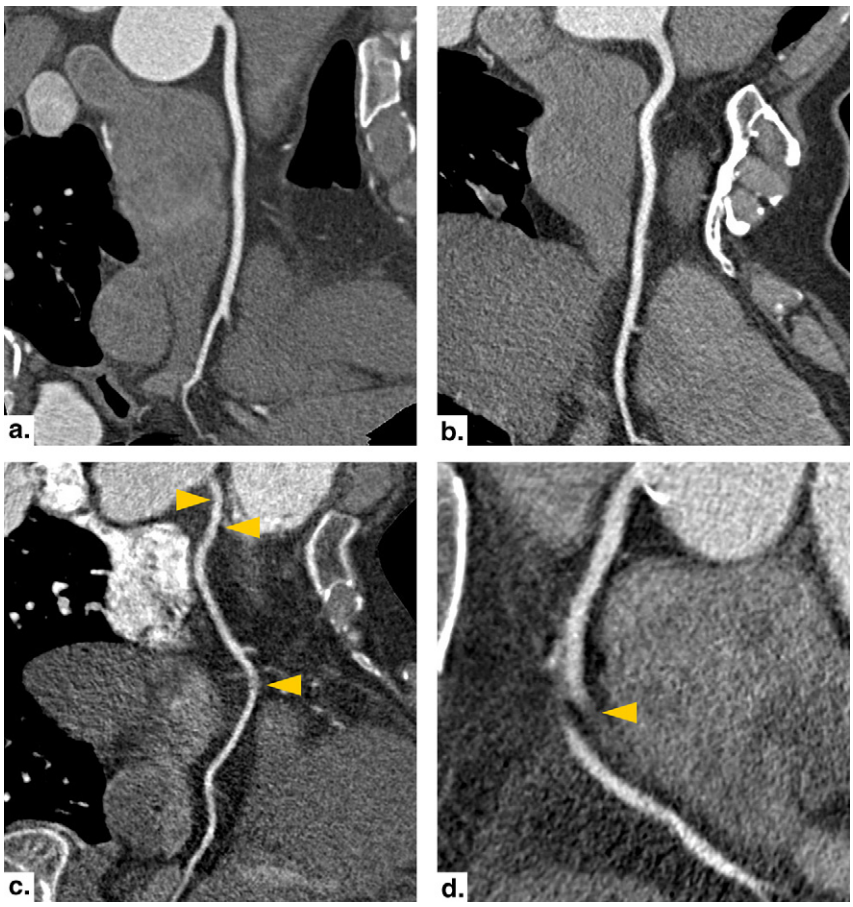

Figure 2. Curved multiplanar reconstruction images of the right coronary artery (RCA) from 4 patients acquired in prospectively gated step and shoot (PGSS) mode with 256-slice computed tomography. The images illustrate the use of the semiquantitative 4-point image quality score. **(a)** Diastolic image (78% of R-R interval) in a patient with a mean heart rate (MHR) = 62 ± 0.8 beats/min, shows no motion artifact in all RCA segments (score 1). **(b)** Diastolic image (78% R-R interval) in a patient with a MHR = 57 ± 1.3 beats/min, shows mild motion artifacts (score 2) that cause mild blurring of the RCA wall. **(c)** Diastolic image (80% of R-R interval) in a patient with a MHR = 71 ± 0.7 beats/min, shows moderate motion artifacts (score 3) in the proximal and middle segments of the RCA, with moderate blurring of the vessel outline. **(d)** Diastolic image (72% R-R interval) in a patient with MHR = 71 ± 2.4 beats/min, shows severe artifacts (score 4) with discontinuity of the middle segment of RCA causing nondiagnostic image quality.

current modulation that allows delivering of the full tube current only during selected phases of the cardiac cycle, resulting in dose savings of up to 50% (21) with no significant degradation of quantitative assessment (22). Compared to studies particularly with DSCT with scan durations of 14–16 seconds (23,24), scan times with the 256-slice CT were 70–75% shorter (ie, 3.9–4.9 seconds). Scan duration reductions of approximately 50% as compared to 40.0 mm z-coverage of 64-slice CT are possible (2,6–8,12). The reduction in axial shots (2–3 for RGH) to cover the necessary cardiac anatomy using the 256-slice CT with 80 mm z-coverage is a significant compared to the 64-slice CT and DSCT (2,6–9,12,23,24). Although still requiring more than one axial step with z-coverage greater than 80 mm, the potential stair-step artifact has not been associated with nondiagnostic images as noted in previous studies with 40.0 mm of z-coverage (6–8,12–16,23–25). To decrease radiation, the 256-slice CT can automatically choose an optimal detector collimation to minimize the number of steps and reduce the amount of z-overscan. In addition, the real-time arrhythmia management of the 256-slice scanner pauses x-ray acquisition on detection of ectopy. This further reduces radiation dose as exposure only occurs during normal sinus rhythm.

Prior studies have indicated that for HRs <75 beats/min, 0.8–5 % coronary segments were considered to be nonevaluative when using 64- and 128-slice CT and DSCT (6–8,12,16,23–27). However, with the 256-slice CT in this study, only 0.1% of coronary segments were nonevaluative using the PGSS technique, as compared to 1.4% as reported by Earls et al for a 64-slice CT (6), indicating that PGSS may be particularly favorable for 256-slice CT because of its higher temporal resolution as compared to 64-slice CT.

The advancing development of 320-slice CT now makes imaging the whole heart in a single snapshot feasible. That approach may reduce the radiation exposure by four- to five-fold as it avoids overscanning (ie, overlapping rotations for helical cardiac scan with no dose modulation) and overranging (ie, the extra two rotations necessary at the beginning and the end of CT scans). Dewey et al showed that a median dose of 4.2 mSv can be achieved using 320-slice CT while still maintaining comparable accuracy of coronary angiography (28). Although optimizing the acquisition parameters may further reduce the dose, this scanner is still with limited availability and its image quality, radiation dose and diagnostic accuracy awaits more head-to-head comparison with other existing CT scanners.

The main limitation of this study is the lack of validation (ie, comparison between the two acquisition techniques with the conventional coronary angiography). Other limitations should also be taken into consideration, such as, in this retrospective study of clinical cases, some parameters were not strictly regulated and image quality scoring was subjective

TABLE 2. RGH and PGSS Image Quality Scores for All Segments

	RGH				PGSS			
Segment*	Score 1 (%)	Score 2 (%)	Score 3 (%)	Score 4 (%)	Score 1 (%)	Score 2 (%)	Score 3 (%)	Score 4 (%)
1	57.1 (72/126)	42.1 (53/126)	0.8 (1/126)	0.0 (0/126)	58.4 (73/125)	39.2 (49/125)	2.4 (3/125)	0.0 (0/125)
2	21.4 (27/126)	59.5 (75/126)	19.0 (24/126)	0.0 (0/126)	26.4 (33/125)	54.4 (68/125)	18.4 (23/125)	0.8 (1/125)
3	56.3 (67/119)	42.9 (51/119)	0.8 (1/119)	0.0 (0/119)	53.8 (64/119)	45.4 (54/119)	0.8 (1/119)	0.0 (0/119)
4	42.7 (50/117)	54.7 (64/117)	2.6 (3/117)	0.0 (0/117)	52.9 (63/119)	46.2 (55/119)	0.8 (1/119)	0.0 (0/119)
5	87.2 (109/125)	12.8 (16/125)	0.0 (0/125)	0.0 (0/125)	80.0 (100/125)	19.2 (24/125)	0.8 (1/125)	0.0 (0/125)
6	78.6 (99/126)	21.4 (27/126)	0.0 (0/126)	0.0 (0/126)	75.2 (94/125)	22.4 (28/125)	2.4 (3/125)	0.0 (0/125)
7	53.6 (67/125)	46.4 (58/125)	0.0 (0/125)	0.0 (0/125)	54.4 (68/125)	44.8 (56/125)	0.8 (1/125)	0.0 (0/125)
8	32.8 (41/125)	64.0 (80/125)	3.2 (4/125)	0.0 (0/125)	31.2 (39/125)	64.0 (80/125)	4.8 (6/125)	0.0 (0/125)
9	48.4 (60/124)	50.0 (62/124)	1.6 (2/124)	0.0 (0/124)	62.4 (78/125)	36.8 (46/125)	0.8 (1/125)	0.0 (0/125)
10	41.5 (27/65)	55.4 (36/65)	3.1 (2/65)	0.0 (0/65)	58.1 (54/93)	39.8 (37/93)	2.2 (2/93)	0.0 (0/93)
11	64.0 (80/125)	36.0 (45/125)	0.0 (0/125)	0.0 (0/125)	67.7 (84/124)	29.8 (37/124)	2.4 (3/124)	0.0 (0/124)
12	33.6 (39/116)	64.7 (75/116)	1.7 (2/116)	0.0 (0/116)	41.4 (48/116)	55.2 (64/116)	3.4 (4/116)	0.0 (0/116)
13	40.2 (45/112)	58.0 (65/112)	1.8 (2/112)	0.0 (0/112)	43.1 (47/109)	53.2 (58/109)	3.7 (4/109)	0.0 (0/109)
14	39.7 (27/68)	57.4 (39/68)	2.9 (2/68)	0.0 (0/68)	32.9 (23/70)	61.4 (43/70)	5.7 (4/70)	0.0 (0/70)
15	62.5 (5/8)	37.5 (3/8)	0.0 (0/8)	0.0 (0/8)	60.0 (3/5)	40.0 (2/5)	0.0 (0/5)	0.0 (0/5)
16	47.6 (20/42)	52.4 (22/42)	0.0 (0/42)	0.0 (0/42)	75.0 (42/56)	23.2 (13/56)	1.8 (1/56)	0.0 (0/56)
All segments	50.6 (835/1649)	46.8 (771/1649)	2.6 (43/1649)	0.0 (0/1649)	54.2 (913/1686)	42.3 (714/1686)	3.4 (58/1686)	0.1 (1/1686)

PGSS, prospectively gated step and shoot; RGH, retrospectively gated helical.

Data in parentheses are raw data used to calculate the percentage. Image quality score obtained at best R-R interval: score 1, no motion artifacts; score 2, mild motion artifacts; score 3, moderate motion artifacts; score 4, severe motion artifacts.

*Right coronary artery included segments 1–4; left anterior descending coronary artery included segments 5–10; left circumflex coronary artery included segments 11–15.

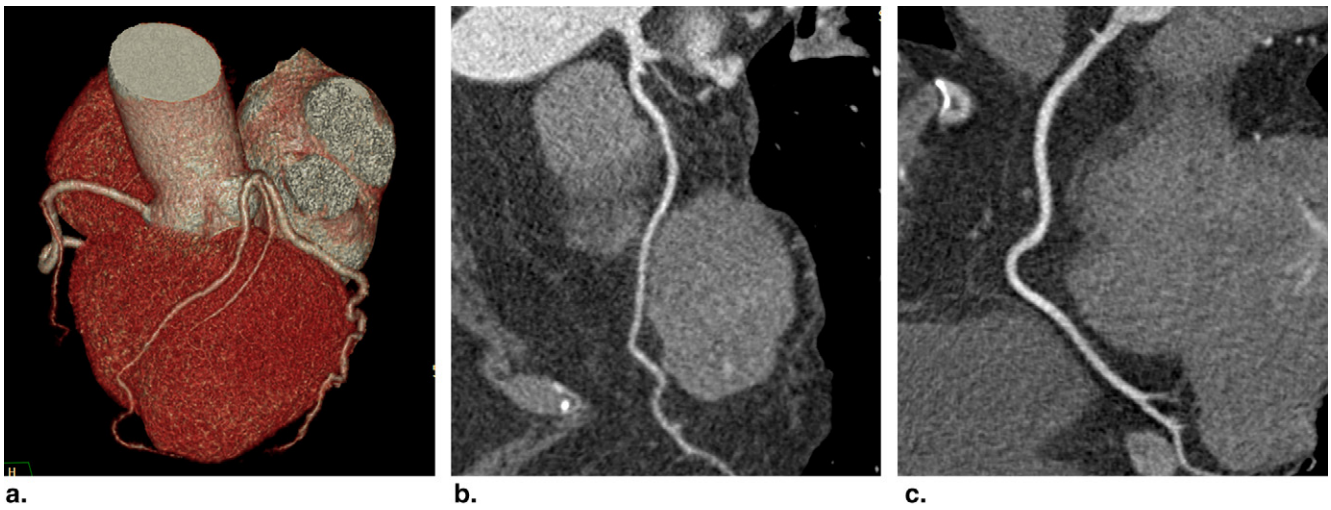

Figure 3. Systolic images (52% R-R interval) from 256-slice computed tomography in retrospectively gated helical (RGH) mode for a patient with mean heart rate = 95 beats/min, heart rate variability (HRV) = 0.9 beats/min, effective dose = 13.01 mSv. **(a)** Three-dimensional volume-rendered image shows well opacified right coronary artery, left anterior descending coronary artery, and left circumflex coronary artery. **(b, c)** Curved multiplanar reformatted images show only mild motion artifacts that cause mild blurring of the left anterior descending coronary artery and right coronary artery wall.

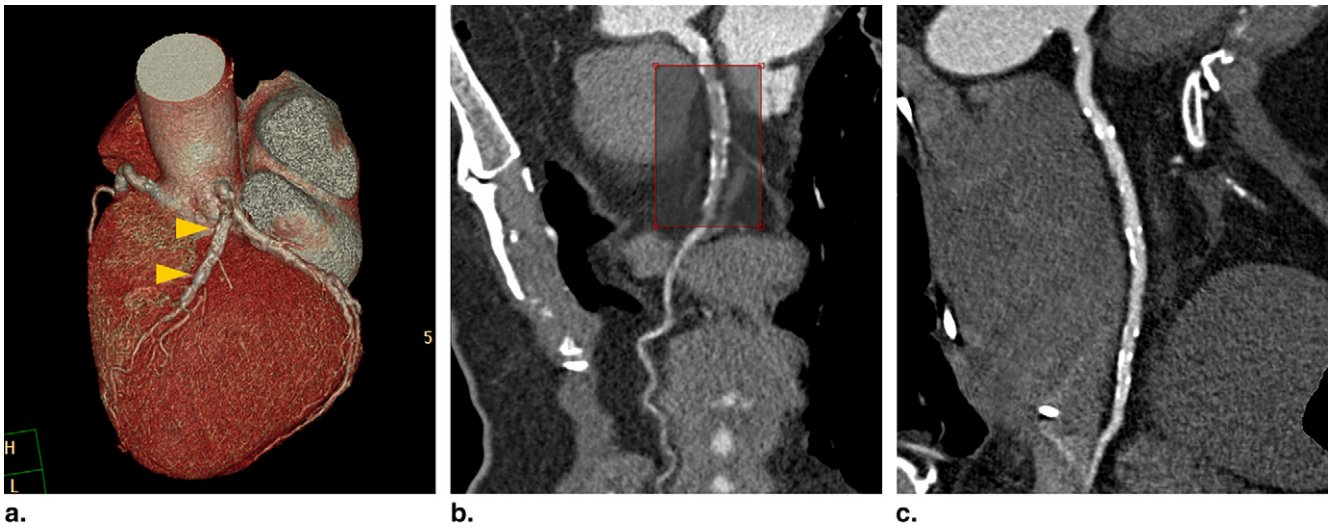

Figure 4. Three 256-slice computed tomography images acquired in prospectively gated step and shoot mode for a patient with mean heart rate = 60 beats/min, heart rate variability = 4.0 beats/min, effective dose = 4.2 mSv. **(a)** Three-dimensional volume-rendered images show well opacified right coronary artery, left anterior descending coronary artery (LAD), and left circumflex coronary artery. A metallic stent placed in proximal segment of the LAD is shown (arrows). Curved multiplanar reformatted images show **(b)** metallic stent placed in proximal segment of LAD and **(c)** multiple calcified plaques in the right coronary artery with mild stenosis (<50%).

and thus susceptible to observer bias. For example, in terms of gender, there are significantly more males in the RGH group than in the PGSS group. The current PGSS implementation itself has inherent limitations because of the lack of multisector reconstruction capability. In its current version, a mid-diastolic trigger centered at 75% of the R-R interval is used to align the imaging window with diastole for patients with HRs ≤75 beats/min. At a higher HR (>75 beats/min), an end-systolic imaging window centered at 40% of the R-R interval can be used to image the heart in a rest period composed of the reduced ejection, protodiastole ejection, and isovolumetric relaxation time phases. Also, studies have shown that PGSS technique is more suitable for patients with lower HR (7,29). Thus, for the benefits of the patients, we did not investigate the robustness of the PGSS technique for patients with HRs >75 beats/min, which may introduce bias that favors image quality of the PGSS group. Additionally, for image quality evaluation, we took into account only the presence of coronary motion artifacts. Other image quality indices, such as signal-to-noise ratio or calcium-related blooming artifacts were not evaluated in this study. Last, a detailed comparison of radiation dose of PGSS

TABLE 3. Comparison of Image Quality for RGH and PGSS Techniques

	RGH		PGSS	Difference Between Techniques*	
Coronary Vessel	Group A1 (All HRs, n = 126)	Group A2 (HR ≤75, n = 84)	Group B (HR ≤75, n = 126)	Group A1 vs. B	Group A2 vs. B
Overall image quality	1.522 ± 0.317	1.472 ± 0.313	1.500 ± 0.374	0.023 (0.23)	-0.028 (0.96)
RCA	1.623 ± 0.442	1.571 ± 0.431	1.580 ± 0.465	0.043 (0.39)	-0.009 (0.95)
LAD	1.429 ± 0.331	1.388 ± 0.328	1.424 ± 0.377	0.005 (0.45)	-0.036 (0.86)
LCX	1.556 ± 0.430	1.467 ± 0.446	1.547 ± 0.469	0.009 (0.68)	-0.080 (0.26)

HR, heart rate; LAD, left anterior descending coronary artery; LCX, left circumflex coronary artery; PGSS, prospectively gated step and shoot; RCA, right coronary artery; RGH, retrospectively gated helical.

Group A1 includes all patients scanned by RGH; group A2 are patients with HR <75 beats/min, scanned by RGH; group B includes patients with HR <75 beats/min, scanned by PGSS. Group data are presented as mean ± standard deviation.

*Data of group comparisons are presented as differences between means of image quality scores and numbers in parentheses are P values calculated from Wilcoxon signed-rank test.

and RGH with ECG-triggered tube current modulation, and the correlation between BMI and motion artifacts are beyond the scope of this study.

In conclusion, with the 256-slice scanner, more than 50% of segments received the highest imaging score for both the PGSS and RGH technique, and the overall image quality scores for RGH and PGSS groups were 1.522 ± 0.317 and 1.500 ± 0.374, respectively. There was no significant difference in image quality between the two groups for all three coronary vessels. Although providing similar image quality as RGH for patients with prescan HR >70 beats/min, PGSS for patients with prescan HR <70 beats/min was associated with a 62% reduction in effective radiation dose. Further study to confirm the diagnostic accuracy as compared to coronary artery angiography is warranted.

REFERENCES

1. Kocinaj D, Cioppa A, Ambrosini G, et al. Radiation dose exposure during cardiac and peripheral arteries catheterization. Int J Cardiol 2006; 113: 283–284.
2. Klass O, Jeltsch M, Feuerlein S, et al. Prospectively gated axial CT coronary angiography: preliminary experiences with a novel low-dose technique. Eur Radiol 2009; 19:829–836.
3. Mori S, Nishizawa K, Kondo C, et al. Effective doses in subjects undergoing computed tomography cardiac imaging with the 256-multislice CT scanner. Eur J Radiol 2008; 65:442–448.
4. Gerber TC, Kuzo RS, Karstaedt N, et al. Current results and new developments of coronary angiography with use of contrast-enhanced computed tomography of the heart. Mayo Clin Proc 2002; 77:55–71.
5. Morin RL, Gerber TC, McCollough CH. Radiation dose in computed tomography of the heart. Circulation 2003; 107:917–922.
6. Earls JP, Berman EL, Urban BA, et al. Prospectively gated transverse coronary CT angiography versus retrospectively gated helical technique: improved image quality and reduced radiation dose. Radiology 2008; 246:742–753.
7. Husmann L, Valenta I, Gaemperli O, et al. Feasibility of low-dose coronary CT angiography: first experience with prospective ECG-gating. Eur Heart J 2008; 29:191–197.
8. Shuman WP, Branch KR, May JM, et al. Prospective versus retrospective ECG gating for 64-detector CT of the coronary arteries: comparison of image quality and patient radiation dose. Radiology 2008; 248: 431–437.
9. Gutstein A, Wolak A, Lee C, et al. Predicting success of prospective and retrospective gating with dual-source coronary computed tomography angiography: development of selection criteria and initial experience. J Cardiovasc Comput Tomogr 2008; 2:81–90.
10. Weigold WG, Olszewski ME, Walker MJ. Low-dose prospectively gated 256-slice coronary computed tomographic angiography. Int J Cardiovasc Imaging 2009; 25:217–230.
11. Alkadhi H, Stolzmann P, Desbiolles L, et al. Low-dose, 128-slice, dual-source CT coronary angiography: accuracy and radiation dose of the high-pitch and the step-and-shoot mode. Heart 2010; 96:933–938.
12. Hirai N, Horiguchi J, Fujioka C, et al. Prospective versus retrospective ECG-gated 64-detector coronary CT angiography: assessment of image quality, stenosis, and radiation dose. Radiology 2008; 248:424–430.
13. Xu L, Yang L, Zhang Z, et al. Low-dose adaptive sequential scan for dual-source CT coronary angiography in patients with high heart rate: Comparison with retrospective ECG gating. Eur J Radiol 2009 Jul 10 [Epub ahead of print].
14. Austen WG, Edwards JE, Frye RL, et al. A reporting system on patients evaluated for coronary artery disease. Report of the Ad Hoc Committee for Grading of Coronary Artery Disease, Council on Cardiovascular Surgery, American Heart Association. Circulation 1975; 51:5–40.
15. Leschka S, Wildermuth S, Boehm T, et al. Noninvasive coronary angiography with 64-section CT: Effect of average heart rate and heart rate variability on image quality. Radiology 2006; 241:378–385.
16. Flohr TG, McCollough CH, Bruder H, et al. First performance evaluation of a dual-source CT (DSCT) system. Eur Radiol 2006; 16:256–268.
17. Efstathopoulos EP, Kelekis NL, Pantos I, et al. Reduction of the estimated radiation dose and associated patient risk with prospective ECG-gated 256-slice CT coronary angiography. Phys Med Biol 2009; 54:5209–5222.
18. Weustink AC, Mollet NR, Pugliese F, et al. Optimal electrocardiographic pulsing windows and heart rate: effect on image quality and radiation exposure at dual-source coronary CT angiography. Radiology 2008; 248:792–798.
19. DeFrance T, Dubois E, Gebow D, et al. Helical prospective ECG-gating in cardiac computed tomography: radiation dose and image quality. Int J Cardiovasc Imaging 2010; 2:99–107.
20. Dewey M. Prospective helical acquisition for coronary CT angiography. Int J Cardiovasc Imaging 2010; 26:109–110.
21. Lehmkuhl L, Gosch D, Nagel HD, et al. Quantification of radiation dose savings in cardiac computed tomography using prospectively triggered mode and ECG pulsing: a phantom study. Eur Radiol 2010; 20:2116–2125.
22. Mahnken AH, Bruners P, Schmidt B, et al. Left ventricular function can reliably be assessed from dual-source CT using ECG-gated tube current modulation. Investig Radiol 2009; 44:384–389.
23. Scheffel H, Alkadhi H, Leschka S, et al. Low-dose CT coronary angiography in the step-and-shoot mode: diagnostic performance. Heart 2008; 94:1132–1137.
24. Stolzmann P, Leschka S, Scheffel H, et al. Dual source CT in step-and-shoot mode: noninvasive coronary angiography with low radiation dose. Radiology 2008; 249:71–80.
25. Hausleiter J, Meyer T, Hadamitzky M, et al. Radiation dose estimates from cardiac multislice computed tomography in daily practice: impact of different scanning protocols on effective dose estimates. Circulation 2006; 113:1305–1310.

26. Matt D, Scheffel H, Leschka S, et al. Dual-source CT coronary angiography: image quality, mean heart rate, and heart rate variability. AJR Am J Roentgenol 2007; 189:567–573.
27. Herzog BA, Husmann L, Burkhard N, et al. Accuracy of low-dose computed tomography coronary angiography using prospective electrocardiogram-triggering: first clinical experience. Eur Heart J 2008; 29:3037–3042.
28. Dewey M, Zimmermann E, Deissenrieder F, et al. Noninvasive coronary angiography by 320-row computed tomography with lower radiation exposure and maintained diagnostic accuracy: comparison of results with cardiac catheterization in a head-to-head pilot investigation. Circulation 2009; 120:867–875.
29. Chazen JL, Prince MR, Yip R, et al. Post-CABG coronary CT angiography radiation dose and graft image quality in retrospective versus prospective ECG gating. Acad Radiol 2010; 17:1122–1127.